Construction and Building Materials 436 (2024) 136922

Contents lists available at ScienceDirect

Construction and Building Materials

journal homepage: www.elsevier.com/locate/conbuildmat

Impact of nanohybrid on the performance of non-reinforced biocomposites and glass-fiber reinforced biocomposites: Synthesis, mechanical properties, and fire behavior

Xiang Ao [a,b], Robert Crouse [c], Carlos González [a,b], De-Yi Wang [a,d,*]

[a] IMDEA Materials Institute, C/Eric Kandel, 2, Getafe, Madrid 28906, Spain
[b] E.T.S. de Ingenieros de Caminos, Universidad Politécnica de Madrid, Calle Profesor Aranguren 3, Madrid 28040, Spain
[c] Department of Mechanical Engineering, Michigan State University, 428 South Shaw Lane, East Lansing, MI 48824, USA
[d] Escuela Politécnica Superior, Universidad Francisco de Vitoria, Ctra, Pozuelo-Majadahonda Km 1, 800, Pozuelo de Alarcón, Madrid 28223, Spain

ARTICLE INFO

Keywords:
Glass fiber-reinforced biocomposites
Fire mechanical integrity
Flame retardancy

ABSTRACT

Biobased polymers are gaining increasing popularity particularly within key industries such as construction and building materials. However, glass fiber-reinforced polymer composites (GFRCs) based on biobased epoxy thermoset are inherently vulnerable against fire, producing huge fire hazards and eventually loss of structural integrity. In this work, a cobalt-based nanohybrid filler (CNH) was designed and synthesized to act as a high-performance synergist for biobased epoxy resin when combined with phosphorous flame retardants (FRs). An optimized formulation was found, resulting in a flame-retarded epoxy resin with a limiting oxygen index (LOI) value of 39.7 % and a V 0 rating in the vertical burning test. The GFRCs were then fabricated with optimized formulation. Interestingly, results showed that the percentage of peak heat release (PHRR) rate reduction was retarded from 74 % for the mixed resin to 36 % for GFRCs, potentially due to the interference of glass fiber. The optimized laminate with CNH showed improved mechanical properties at ambient temperature. Additionally, delayed time-to-failure values were found when sample coupons with CNH were subjected to a constant axial force loading while being ignited and burning, indicating higher resistance against fire for mechanical integrity.

1. Introduction

To effectively address climate change and the global issue of polymer pollution, it's imperative to implement a shift from relying on fossil-based materials and energy to promoting the bio-based materials economy, particularly within key industries such as construction and building sectors. [1,2] By extracting compounds from biomass feedstocks and converting them into bio-based polymers [3], vigorous efforts are being conducted to explore their full potential to replace petroleum-derived polymers such as in engineering materials application of glass fiber-reinforced polymer composites (GFRCs). [4] As one of the popular choices for polymer matrices, various types of biobased epoxy thermosets have been proposed and investigated for a promising candidate with such as ideal thermomechanical properties. [5] Various resources such as bio-based monomeric phenols from lignin and epichlorohydrin derived from glycerol (co-product of biofuel product) have been proposed to chemical substitutes for high-performance epoxy resin, aiming to reduce the carbon footprint and improve the sustainability of GFRCs.[6–10]

Nevertheless, the inherent vulnerability to fire remains a bottleneck for biobased epoxy resin composites, limiting their applications in high-performance GFRCs. [9,11] In order to reduce their flammability, flame-retardant moieties must be introduced by incorporating them into the polymer composites. [12,13] Among various types of flame retardants (FRs), phosphorus-based FRs have gained popularity as candidates for flame-retarded epoxy resins [14–17] to replace the traditional halogenated FRs which posed significant risk to human lives and the environment. [18] Ammonium polyphosphate (APP), as an inorganic salt consisting of polyphosphoric acid and ammonia, has been a promising candidate as an acid source and fuel dilution agent in flame retarded polymers with easy of processability, low cost and toxicity. By controlling polymer chain length and branching, APP has been used as a popular candidate for tailoring the fire safety of a wide variety of thermoplastic and thermoset either by coating or physically blending

* Corresponding author at: IMDEA Materials Institute, C/Eric Kandel, 2, Getafe, Madrid 28906, Spain.
E-mail address: deyi.wang@imdea.org (D.-Y. Wang).

https://doi.org/10.1016/j.conbuildmat.2024.136922
Received 20 February 2024; Received in revised form 20 May 2024; Accepted 3 June 2024
Available online 10 June 2024

comparing with other P-containing flame retardants. [18,19] However, APP generally needs to be improved either by surface modifications [20] and/or by blending with other synergists to enhance its matrix compatibility, water solubility and most importantly efficacy.

Metal organic framework (MOF) and their derived nanohybrids have been proposed to enhance fire retardancy and smoke suppression through catalytic oxidation and char formations. [21,22] The versatile compositions and abundant structures of MOF-derivatives offer great design flexibility for flame-retarded epoxy resin. Zhang et al. [23] prepared a zirconium-based MOF with molybdenum disulfide into a nanohybrid filler (UiO66-MoS_2) and explored its flame retardancy in epoxy resin. With 2 wt% of this nanohybrid, the limiting oxygen index (LOI) of the modified resin was increased by 16 %, and the vertical burning test (UL 94) improved to a V1 rating. The cone calorimeter results (CCT) demonstrated a 46 % peak heat release rate (PHRR) value for 2 wt% loaded resin. Hou et al. [24] designed a multielement FRs system by coupling cobalt-based MOF, polyhedral oligomeric silsesquioxane (POSS) and diphenylphosphine into a hybrid filler named MPOFs-P. The results showed that with 2 wt% of MPOFs-P, the modified resin could reach a V0 rating in the UL 94 test, with an increase in LOI value by around 22 %. CCT results showed an increase of char value by 400 % and a decrease of PHRR value by 50 %. The cobalt-based MOF and its derived nanohybrids have shown promising performance in recent years especially in aromatic ring rich epoxy resin system [25,26]. However, for GFRCs, especially continuous fiber reinforced polymer composite, the mechanical integrity is of the same importance as the flame retardancy as suggested by our previous work [27]. Few previous efforts have demonstrated the incorporation of MOF-based derivates in epoxy resin-based polymer composites and evaluated their influence on fire retardants' efficacy and mechanical properties to the best of our knowledge.

Aluminum trihydrate (ATH) as a widely used synthetic mineral FRs has shown potential to as host material for synthesis multi-metal based nanohybrid for flame retardants coating or additive applications. [28,29] Hence, in this work, we designed and synthesized a novel cobalt-based nanohybrid (CNH) by using a facile approach to *in-situ* grow cobalt-based MOF particles on the slab of micro-sized ATH. After verifying the successful synthesis of CNH, this new filler was used as a novel, high-performance synergist with aluminum polyphosphate (APP) based FRs for filled biobased epoxy resin and GFRCs. The efficacy of FRs was screened in epoxy resin to select the optimized formulation for fabricating glass fiber reinforced epoxy composite (GFRP). The flame-retardant mechanisms were investigated and proposed to explain the different behaviors between unreinforced resins composite and GFRCs. Finally, FRs' influence on composites' mechanical properties in both ambient temperature or under simultaneously burning scenario to explore the influence of nanohybrid on the mechanical properties.

2. Materials and methods

Aluminum trihydrate (SB-432) was provided by J.M. Huber Corporation. Cobalt (II) acetate tetrahydrate was purchased from Alfa Aesar. 2-Methylimidazole (2-MIM) was purchased from TCI. Flame retardant (Exolit AP 750) with APP as the main component was kindly provided by Clariant. Type II water was produced by a water purification machine (Wasserlab Automatic plus). Biobased Epoxy resin (Resoltech 1800 ECO) and cycloaliphatic & aliphatic amine curing agent (Hardener 1804 ECO) were purchased from Resoltech, France. The glass fiber based woven fabric (UTE 275 P, plain weave, 275 g/m^2) was purchased from Castro Composites SL.

2.1. Synthesis of synergist CNH

As shown in Scheme 1, a fully dissolved 2-MIM/water with a concentration of 0.224 g/ml solution was prepared by magnetic stirring. After that, ATH was dispersed into a 2-MIM/ DI water solution under an ultrasonic probe (500 W) with an ice bath to form a suspension with ATH concentration being 0.16 g/ml. Meanwhile, Cobalt salt was fully dissolved in DI water with a concentration of 0.12 g/ml by magnetic stirring. Then, the Cobalt salt/water solution was poured into ATH/2-MIM/water suspension under continuous ultrasonic probe dispersing for 10 mins. After that, the suspension was centrifuged several times under 3000 RPM for 5 min to discard the supernatant, washed with methanol, and finally put in a vacuum oven at 70℃ overnight. The resulting solid purple product was crushed into a fine powder before use with an actual yield of 37.2 %.

2.2. Preparation of biobased epoxy resin with APP and CNH

Different weight ratios of APP and CNH were added into the epoxy under 1300RPM for 10 minutes using an overhead stirrer with high-shear disperser blades. After that, a stoichiometric amount of amine hardener was added and mixed for at least 3 minutes. The resulting viscous liquid mixture was degassed in a vacuum chamber at below100 mbar for 10 minutes before being transferred and poured into a silicon resin-based flexible non-stick mold and heat cured according to the temperature program recommended by the supplier in a convection oven (50℃ for 3 hours, then 100℃ for 3 hours). Six FRs filled with epoxy resin were prepared: Pure EP, 20APP/EP,14APP-6CNH/EP,10APP/EP, 7APP-3CNH/EP, 5APP-5CNH/EP according to the details shown in Table 1.

2.3. Preparation of GFRP with APP and CNH

GFRP laminates were prepared using hand layup methods. The glass fiber-based fabric was applied and impregnated using the aforementioned liquid mixture using hand rollers. Ten layers of glass fiber woven fabric were stacked $[0/90]_{5\,s}$. The stacked impregnated fabrics were then transferred to a hot press machine to cure at around 1.3 bar following a temperature program of 50℃ for three hours and 100℃ for three hours to obtain a quasi-isotropic laminate. The laminate was inspected for minimal defects by a nondestructive ultrasonic scan (Figure S1). The resulting laminate has a thickness of around 2.3 mm and a fiber weight ratio of around 63 %. Finally, the laminates were machined to get the desired dimension testing. Three laminates were prepared: Pristine GFRP, 20APP/GFRP and 14APP-6CNH/GFRP.

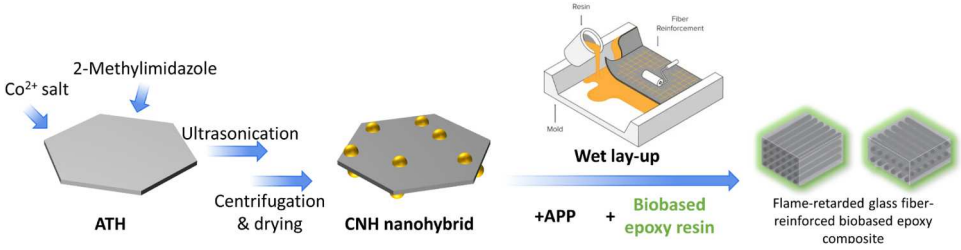

Scheme 1. Facile synthesize CNH and its use in fabrication of GFRP.

Table 1
Formulations of epoxy resin with different ratios of FRs and their LOI value and UL 94 rating (3.2 mm).

Sample	APP (wt%)	CNH (wt%)	Epoxy (wt%)	Hardener(wt%)	LOI (%)	UL 94 (3.2 mm)
Pure EP	0	0	79.4	20.6	21.7	NR
20APP/EP	20	0	63.5	16.5	24.2	NR
14APP-6CNH/EP	14	6	63.5	16.5	39.7	V0
10APP/EP	10	0	71.5	18.5	22.9	NR
7APP-3CNHEP	7	3	71.5	18.5	28.9	V2
5APP-5CNH/EP	5	5	71.5	18.5	25.1	NR

2.4. Characterizations and measurements

Scanning electron microscopy (SEM) and EDS were carried out on a scanning electron microscope (Apero 2, Thermo Fisher). X-ray diffraction (XRD) patterns of the CNH fillers were obtained in reflection mode using a Philip X'Pert PRO diffractometer with Cu Kα (λ=0.1542 nm) and Ni filter. The thermogravimetric analysis (TGA) curves under air and nitrogen atmosphere were measured with an instrument from TA Instruments (Q50) at a temperature ramp speed of 20℃/min. TG-IR test was carried out on a infrared spectrometers (Nicolet IS 50, Thermo-Fisher) with TGA coupled to screen the volatile products produced during the thermal decomposition of resin mixture in a nitrogen atmosphere at a heating rate of 20 K/min. Optical microscopy was carried out by using optical microscopes (SZX 10 and BX 51, Olympus).

LOI test and UL 94 test for resin samples were measured by following standard of D2863–19 and UL 94. The forced flaming test was carried out on a dual cone calorimeter (Fire Testing Technology, UK) with the sample dimension of 100 mm × 100 mm × 2.3 mm in the horizontal direction and positioned 25 mm away from a heat flux of 50 kW/m^2 to the ISO 5660–1:2015 standard.

Following the ASTM D3039/D3039M-08 standard, the tensile behaviour of the composite at ambient temperature was measured using a universal testing frame (3300 series, Instron) equipped with a 130 kN load cell. Deformation was measured by a 12.5 mm gauge length standard resistive extensometer. Rectangular coupons of 250×25 mm^2 tabbed with glass/epoxy laminates glued by epoxy adhesive during testing were used. Two batches of specimens were prepared for the tests: 20APP/GFRP and 14APP-6CNH/GFRP. After failure, the areas close to the failure surface of the composite coupons were cut and cold-mounted in epoxy resin to prepare for examining failure mechanisms. The samples were subsequently grounded, polished, and gold-sputtered for SEM inspections.

A bench scale accessory for testing the sample coupon under constant axial load and fire conditions was specially designed and mounted on the cone calorimeter. The labscale machine was constructed via a four-pillar load and a load transfer system incorporating a pneumatic actuator and an in-line load cell. The constant load was generated by compressed air through the pneumatic actuator with the adjustment from the pressure regulator. Sample coupons were clamped with wedge grips. The area outside the grip location was covered with a fire-resistant blanket to prevent material thermal softening and coupon slippering during the tests. The results of the individual tests comprise the load level (a given ratio to the maximum strength of the composite) and the time for the coupons to sustain the fire conditions imposed in the cone calorimeter.

3. Results and discussions

3.1. Chemical composition and structure of CNH

The XRD test was employed to screen the crystal structure of CNH. As shown in Fig. 1(a), the cobalt-based MOF showed similar peaks to our previous works. The ATH filler displayed a distinctive high-intensity peak around 20°. After the in-situ growth of cobalt-based MOF on the slab of ATH fillers, the peaks around 7.4°, 10.4°, 12.7° and 18° were present in both cobalt-based MOF and newly synthesized CNH. In addition, the strong intensity of the peak at 18° peak in the CNH sample indicates that ATH is the primary component in the hybrid fillers.

The morphology and composition of CNH were screened by SEM and EDS. In Fig. 1(b) it reveals the morphology of newly formed micronized grain on the slab of ATH fillers which is distinct from the pristine ATH. By comparing the EDS images of three different elements in Fig. 1(c), it is evident that the grown grain on the ATH slab consists of Cobalt elements. In conclusion, the successful synthesis of the MOF and ATH hybrid CNH can be verified from the test results mentioned above.

3.2. Flammability of FR-filled biobased epoxy resin

The flammability of FR-filled biobased epoxy resin is measured by small fire tests such as the LOI and the UL 94 test. As mentioned in the previous section, the low charring pure epoxy resin exhibited a low LOI value of 21.7 and an NR rating in the vertical burning test as shown in Table 1. The introduction of APP solely into the epoxy resin only slightly increased the LOI value to less than 25 % and showed no improvement

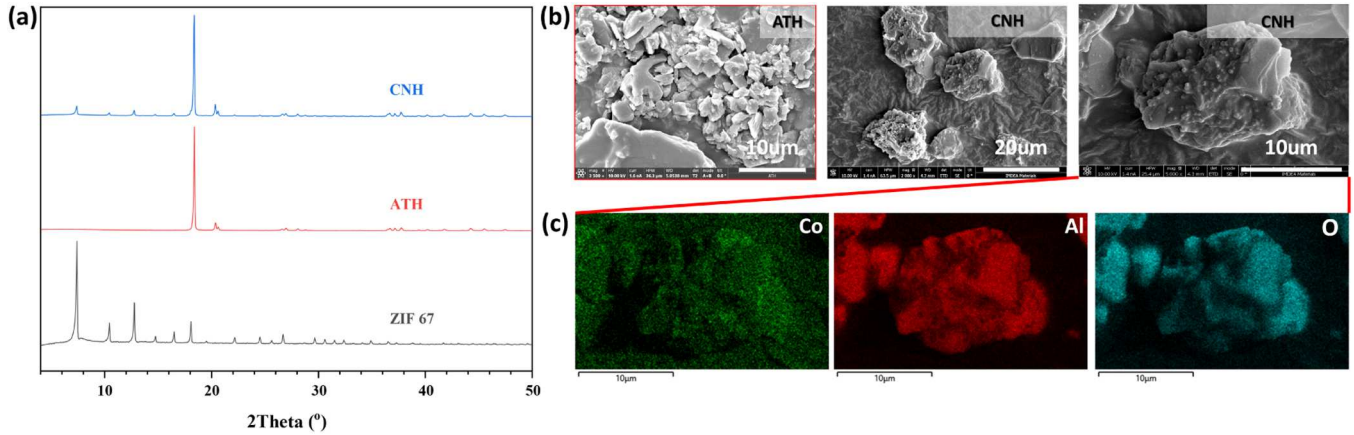

Fig. 1. XRD curves, SEM and EDS images of ATH and CNH.

in the vertical burning performance even with a filler content of 20 wt%. This indicates that APP exhibited poor efficiency in this kind of biobased epoxy resin, which has low viscosity and low charring capabilities.

When the total amount of FR fillers was set as 10 wt%, the optimized ratio between APP and CNH was explored. After replacing parts of APP with CNH synergists, the LOI value increased by 33 % when the ratio of APP to CNH was 7:3. However, when the ratio of CNH was further increased, the LOI value decreased, indicating that insufficient APP will retard the intumescent effects. Hence, an optimized ratio of 7:3 between APP and CNH was found. Due to the V-0 rating not being reached with 10 wt% of total loading, a higher 20 wt% of total loading was tested, and it was found that the LOI value increased by more than 80–39.7 % with a V-0 rating for vertical burning tests. Hence, this formulation was selected for the further preparation of glass fiber-reinforced biobased epoxy composites.

3.3. Combustion behavior of flame retarded biobased epoxy resin

The influence of the filler ratio and content of APP and CNH on the heat and smoke release behavior of biobased epoxy resin was evaluated using a Cone calorimeter, as shown in Fig. 2 and Table 2. As can be seen in Fig. 2, the addition of APP alone reduced the peak heat release rate (PHRR) and total heat release (THR) by more than 40 % and 32 %, respectively. In terms of smoke release, 10APP/EP showed minimal change in the peak smoke release rate (PSRR) but decreased the total smoke production (TSR) by 19.8 %. The introduction of APP didn't drastically change the shape of the HRR curve compared with Pure EP. Both samples displayed a thermally thin type of heat release characterized by a main sharp peak which can be attributed to the failed formation of protective char during the combustion process. [30]

Nevertheless, the introduction of cobalt-containing CNH led to significant changes in the heat release behavior, as observed in Fig. 2(a). Both CNH-containing samples showed two distinct peaks during the heat release profile and an even lower PHRR value compared to that of 20APP/EP. The maximum average rate of heat emission (MARHE) of CNH-containing samples were lowered too. The formation of a two peak heat release profile is usually derived from the formation of protective, compact char, during the first peak range. During the early stage of combustion, the char formation hinders the heat and mass transfer and prolongs the bulk thermal decomposition, resulting in a lower PHRR. However, due to the thermal oxidation of char and continuous heat conduction from the cone heater, eventually the char protection fails, leading to a second heat release peak.

MOF especially nickel-based MOF have been suggested for contribute to catalytic charring effect in the flame retarded polymeric system by several reviews [21,22]. With this biobased epoxy resin possessed every limited charring capability by itself, the decomposition products of APP acted as an acid source as well as blowing source showed limited intumescent effects due to the lack of carbonizing source. After adding CNH as a synergist, CNH was suggested to demonstrate a strong charring promoting effect, producing more char formation for the intumescent swelling actions. With the release of gas source NH_3 into the gas phase, the binary FRs flame retarded epoxy resin system showed a highly intumescent effect as shown in Figure S1.

It is noteworthy that a lower ratio of APP in 5APP-5CNH/EP would

Table 2
CCT results of Pure GFRP, 20APP/GFRP, 14APP-6CNH/GFRP, 10APP/EP, 7APP-3CNH/EP, 5APP-5CNH/EP, Pure GFRP, 20APP/GFRP and 14APP-6CNH/GFRP.

Sample	T_{ig} (s)	PHRR (kW/m^2)	THR (MJ/m^2)	TSR (m^2/m^2)	MARHE (kW/m^2)	Avg-EHC (MJ/m^2)
Pure EP	42	1266	100.2	24.2	491.4	25.0
20APP/EP	35	544	58.9	14.1	206.1	19.1
14APP-6CNH/EP	37	297	63.8	13.7	163.9	21.3
10APP/EP	30	743	67.7	19.4	325.8	21.7
7APP-3CNH/EP	32	456	66.6	15.0	257.2	19.3
5APP-5CNH/EP	32	659	78.1	16.7	346.4	24.1
Pure GFRP	41	484	31.3	7.8	230	24.5
20APP/GFRP	41	385	35.1	9.0	214	22.3
14APP-6CNH/GFRP	27	309	26.6	7.9	184	21.7

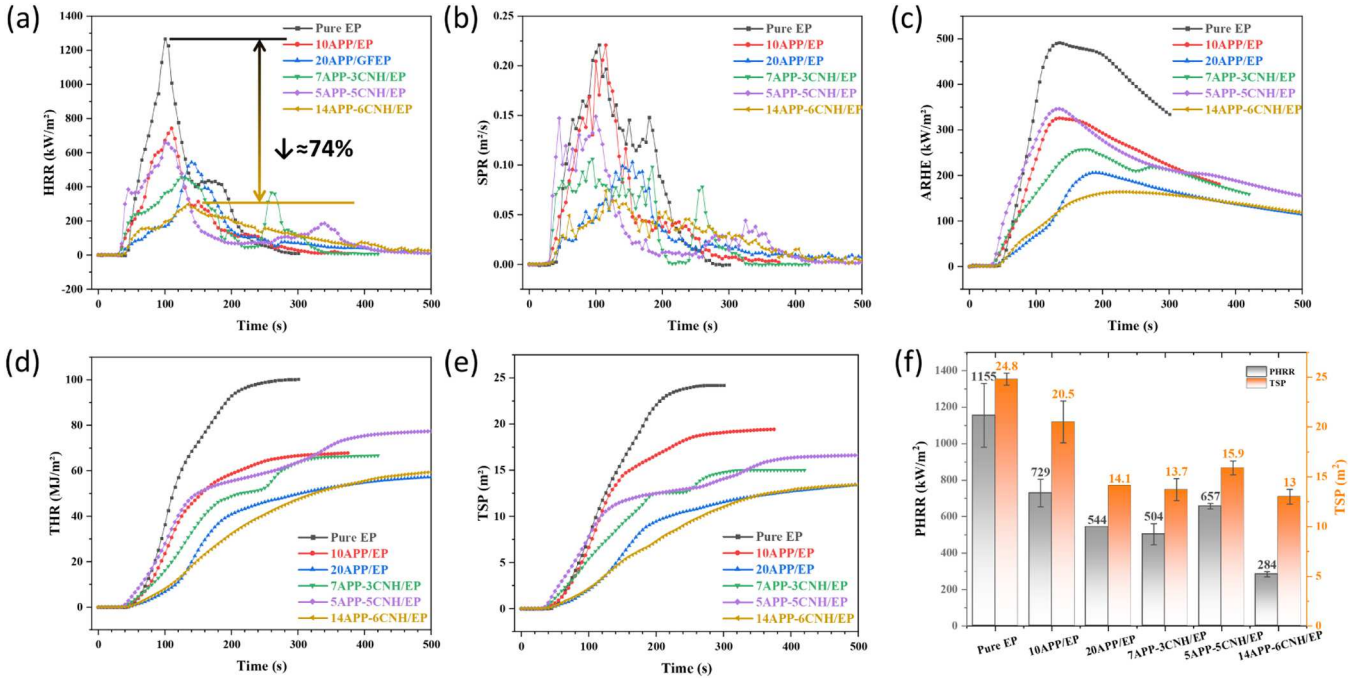

Fig. 2. CCT results curve for heat release (a, c, d), smoke release (b, e) and bar chart (f) for comparing the PHRR and TSP values of Pure EP, 10APP/EP, 7APP-3CNH/EP, 5APP-5CNH/EP, 20APP/EP and 14APP-6CNH/EP.

bring higher PHRR, THR, and TSP values compared to that of 7APP-3CNH/EP, as shown in Fig. 2(f). It suggests that a lower amount of phosphorus acid source leads to an epoxy composite with lower charring capabilities. Since APP primarily functioned as an acid source and gas source in the intumescent system, having too low of an APP ratio with an overloaded content of CNH synergists would lead to poor intumescent effects, thereby compromising fire protective effects. Hence, an optimized ratio of 7:3 between APP and CNH was determined when formulating FRs for biobased epoxy resin.

3.4. Combustion behavior of flame retarded GFRP

The burning behavior of the prepared laminates were evaluated under forced flaming conditions by CCT tests. As can be seen in Table 2 and Fig. 3, the Pure GFRP exhibited a much lower heat and smoke release and a higher residue value compared to the pure biobased epoxy resin, which can be attributed to the dilution effects of the noncombustible glass fiber with a weight ratio of more than 60 wt%. [31] After the introduction of APP fillers, the PHRR value was reduced by 20 %, a much lower reduction compared to the 40 % reduction in PHRR when only 10 wt% APP was added into the pure resin system.

Surprisingly, the THR and TSR values of 20APP/GFRP were higher than those of Pure GFRP. After adding CNH synergists to the laminates, the 14APP-6CNH/GFRP exhibited a smaller reduction in PHRR of 36 % and in MARHE of 20 %. What's more, the THR was lowered by 15 %, and the TSR showed a similar value to that of Pure GFRP. The time-to-ignition (T_{ig}) value was extended to 27 s while the DTG_{max} value of 14APP-6CNH/GFRP was similar to that of 20APP/GFRP as shown in Fig. 3.

3.5. Thermal stability of FR-filled biobased epoxy resin

The thermal stability of CNH synergists and the FR-filled epoxy resin was investigated by TGA in order to understand the fire behavior. As shown in Table S1 and Fig. 4, the Pure EP exemplified a DTG_{max1} at around 340℃ with a low residue value of around 3.7 %, indicating the low charring capability of this biobased epoxy resin. After adding APP and CNH synergists, the residue value significantly increased compared to that of Pure EP, primarily due to the charring promotion provided by the phosphoric acid of APP. However, the DTG_{max} value decreased in both 20APP/EP and 14APP-6CNH/EP, which may be derived from the low thermal stability and the catalytic promotion of thermal decomposition of APP and CNH.

Based on the assumption that no synergistic chemical reactions occurred between the FRs and the polymer matrix, the residue value of the 20APP/EP and 14APP-6CNH/EP were calculated to be 14.2 % and 14.1 %, respectively. The catalytic function of cobalt can be demonstrated by an increase of more than 50 % in the measured residue value compared to the calculated values, suggesting the addition of APP and CNH induced a synergistic reaction with the resin matrix.

3.6. Transfers of FRs behavior from resin to composite

The char residues after the Cone test for different samples are displayed in Fig. 5. Due to the very limited charring capabilities of pure biobased epoxy resin, there was almost no char residue, and the resin was consumed almost entirely during combustion. When 10 wt% APP was introduced into epoxy resin, the resin system exhibited an intermediate intumescent phenomenon with insufficient char integrity after the CCT test in Figure S2 (c). However, after incorporating the CNH synergist, the char expansion was significantly enhanced, as observed in the cross-section digital images. When comparing the influence of different ratios of APP to CNH on the combustion behaviour of resin, the 7APP-3CNH/EP exhibited a more porous inner structure compared to that of 5APP-5CNH/EP as demonstrated in Figure S2 (a, b). The porous structure of the char layer plays a positive role in limiting the mass transfer of combustible volatiles and thermal feedback from the flaming zone into the underlying virgin zone. [32] Hence, the optimized ratio between APP and CNH can provide better fireproofing performance during forced flaming combustion, as shown in Table 2.

When glass fiber reinforcement was introduced into the resin matrix, significant changes were shown in combustion behavior and CCT results. Ideally, glass fiber, an incombustible substance, should hardly influence the chemical aspects of the combustion process. While a

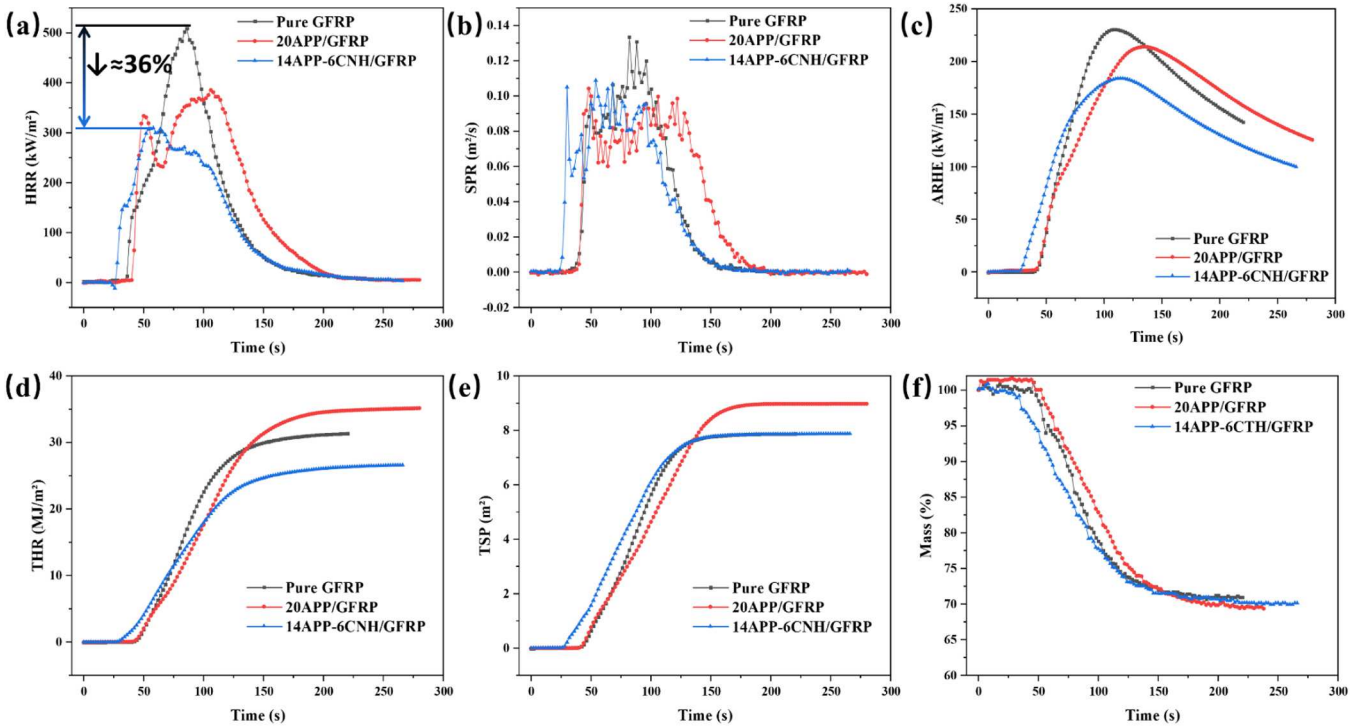

Fig. 3. CCT results curve for heat release (a, c, d), smoke release (b, e) and mass loss (f) of Pure GFRP, 20APP/GFRP and 14APP-6CNH/GFRP.

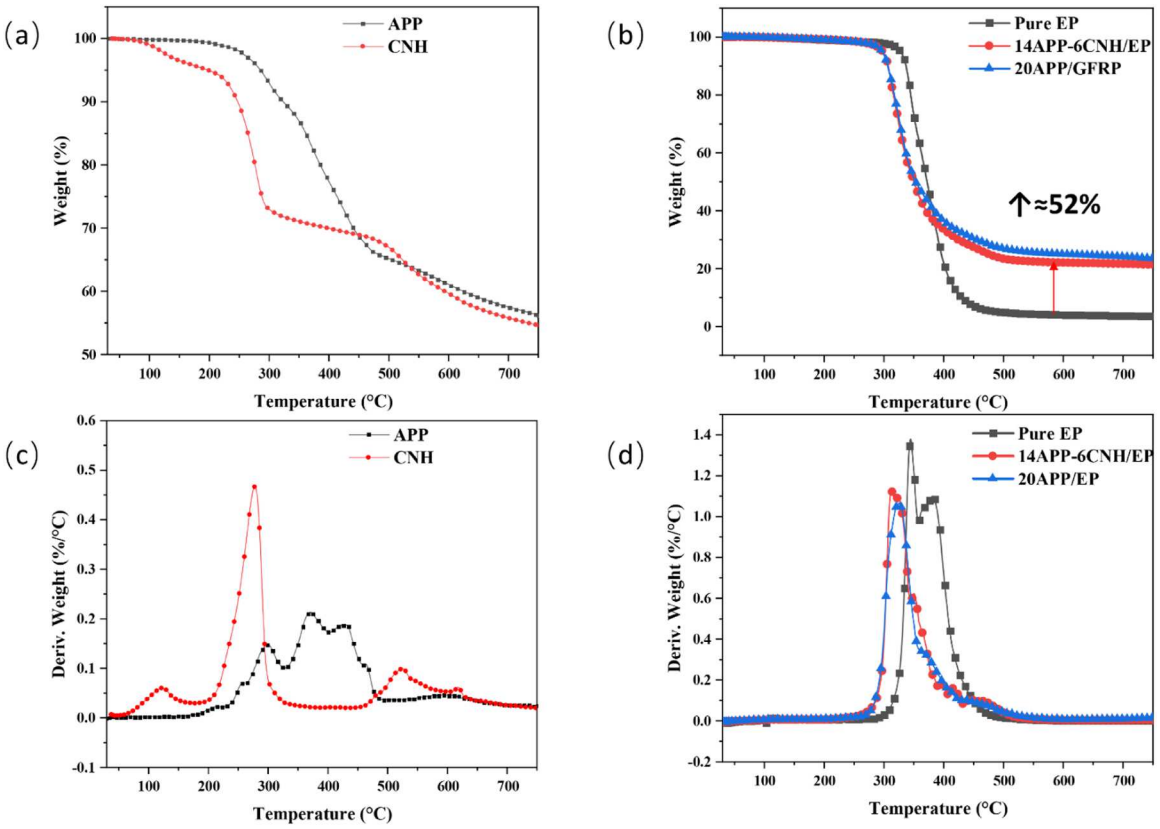

Fig. 4. TGA and DTG curves of CNH and APP in air and N_2. TGA and DTG curves of Pure EP, 14APP-6CNH/EP, 20APP/EP in N_2.

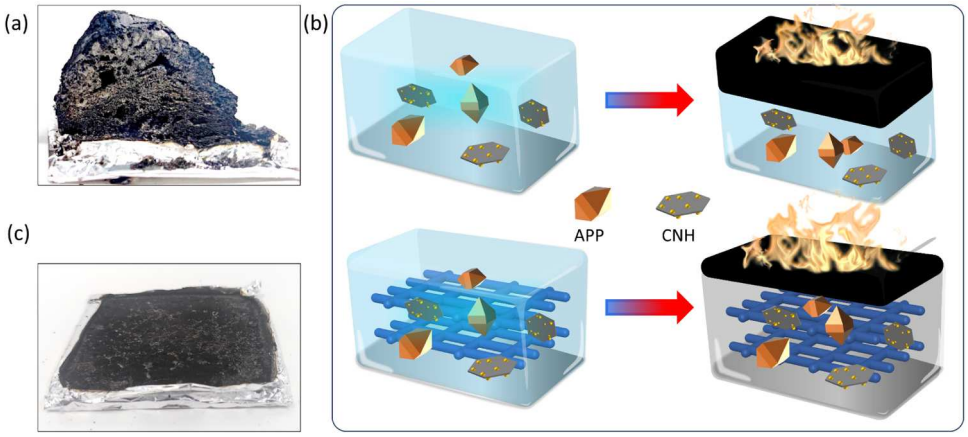

Fig. 5. Cross-section digital images of 7APP-3CNH/EP (a) after cutting the char residue in half. Scheme illustration demonstrating the difference in charring behavior transfer from resin to GFRCs. (b) Digital images of char after CCT tests of 14APP-6CNH/GFRP (c).

reduction of 74 % in PHRR was observed when glass fiber was not introduced into the resin, the efficiency decreased to only 36 % reduction in PHRR for the laminates. In addition, a sharp contrast was observed in the char macro morphology between the bulky resin and polymer composites. The resin with FRs exhibited a distinct intumescent phenomenon, while the laminates after cone tests showed limited charring with very limited intumescent phenomenon.

The change in combustion behavior from Cone results in this study was proposed to partly attribute to the incorporation of glass fiber reinforcement as shown in the schematic illustration of Fig. 5(b). The thermal expansion difference between the glass fiber and polymer matrix tends to induce delamination, as seen by some research.[33,34] Meanwhile, The dense, high weight ratio of glass fabric may create a barrier effect which influenced the macro thermal decomposition process, thereby limiting the reach of critical mass of flammable volatile concentrations. The interplay of two abovementioned possible factors contributed to the complex ignition time variation among the flame retarded epoxy system with and without glass fiber with other parameters such as fire test set-up and etc. as suggested by former reports [35].

As can be seen in Fig. 5(b) and Figure S1, the intumescent phenomenon is significantly retarded in the polymer composites of both 20APP/GFRP and 14APP-6CNH/GFRP. This can be attributed to two factors associated with glass fabric. First, the large surface area of glass fiber inhibits the formation of a compact insulation char layer. Second, the rigid and dense fiber layer restricts the physical expansion of the char layer induced by the release of nonflammable gas. The contribution

of fiber reinforcement also weakens reduction of THR and TSP. These two physiochemical factors retarded the intumescent behavior of the FRs in the GFRCs, thereby demonstrating a transfer of FRs behavior from the resin to the polymer composites as also suggested by former researches [36–38].

In terms of composite laminates, the two flame retarded formulations showed almost close residue mass value at the end of the Cone test in Fig. 3(f) compared to Pure GFRP. Besides, the value of average effective heat of combustion (Avg-EHC) in Table 2 decreased by around 10 % for flame retarded formulation compared to that of Pure GFRP, which indicated a gas phase action. In addition, the release of ammonia may contribute to fuel dilution and heat removal when adding more than 10 wt% of APP flame retardants. Hence, it is possible that this binary FRs formulation may also display a more prominent gas phase flame retardant mechanism in fiberglass composite compared to that of resin with only FRs. By comparing the digital images of Figure S1 (e, f), the sample named 14APP-6CNH showed its glass fiber's surface blanked by char residue while Pure GFRP nearly burned out all resin leaving visible large area dry glass fabric after combustion. These indicated that this APP-CNH composition also demonstrated some condensed phased action in terms of flame retardancy. Hence, the change of matrix system from epoxy resin to fiberglass composite may transfer the APP-CNH binary flame retardants system from a condensed phase dominated intumescent mechanism into a bi-phase flame-retarding actions.

3.7. Mechanical properties of Flame retarded GFRP

The influence of FR fillers on the mechanical properties and stress transfer of the composite coupons was investigated under axial tensile loading on coupons extracted from the manufactured laminates, as observed in the side section of digital photos of the two failed coupons in Fig. 6(b, e). The fracture of the 20APP/GFRP material, Fig. 6(b) is more localized in the area of failure with reduced delamination between the piles. However, the damage is observed far from the fracture surface for the 14APP-6CNH/GFRP material in Fig. 6(e). This fact indicates a global redistribution mechanism opposing the local one observed in the 20APP/GFRP laminate.

To illustrate such mechanisms, metallography images of the failed coupons captured by SEM from locations both close to and away from the failure area. Compared to 14APP-6CNH/GFRP, 20APP/GFRP exhibited less delamination, and a more concentrated failure area, as shown in Fig. 6(a, c). On the other hand, 14APP-6CNH/GFRP exhibited a more globalized failure, indicating a failure process in which energy was dissipated between ply layers during the failure process, as demonstrated in Fig. 6(d, f). The measured tensile test results in Table S2 (modulus and strength) and Fig. 6(g) further supported that 14APP-6CNH/GFRP possessed greater tensile strength and elongation at break compared to 20APP/GFRP. In conclusion, the CNH resulted in additional improvement in mechanical properties by reducing the APP content and enhancing stress transfer during failure, leading to higher tensile properties.

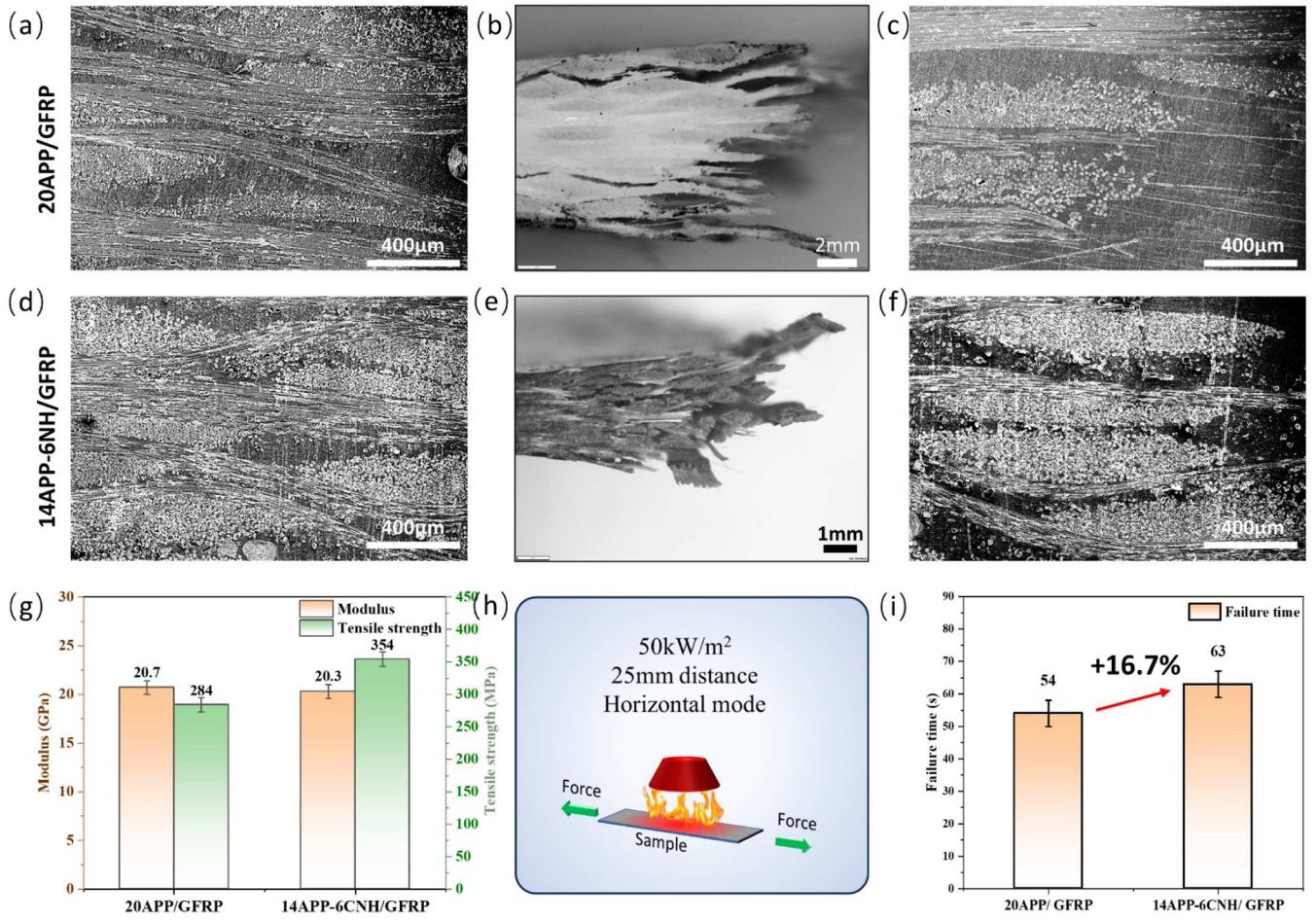

Fig. 6. SEM images from locations away from the failed area of 20APP/GFRP (a) and 14APP-6CNH/GFRP (d). Optical microscope images for the side view of failed coupons of 20APP/GFRP (b) and 14APP-6CNH/GFRP (e). SEM images from locations close to the failed area of 20APP/GFRP (c) and 14APP-6CNH/GFRP (f). (h) Bar chart for comparing Young's modulus and tensile strength of 20APP/GFRP and 14APP-6CNH/GFRP. (g) Schematic illustration for set-up of *in situ* lab scale test for fire machinal properties. (h) Bar chart for comparison of failure time under 25 % failure load and fire for 20APP/GFRP and 14APP-6CNH/GFRP (i).

In this work, we also proposed evaluating the composite's fire mechanical properties by subjecting the composite coupons to fire and tensile stress load. As shown in Fig. 6(h), by constructing a bench scale accessory which can be mounted on Cone Calorimeter, both coupons of 20APP/GFRP and 14APP-6CNH/GFRP were heated and ignited under 50 kW/m^2 while loaded by a tensile stress of 25 % of the corresponding tensile strength. The failure time of the loaded specimens was measured and presented in Table S2 and Fig. 6(i). The modification of the materials increases the time for failure by more than 16 % regarding the samples with only commercial FRs, demonstrating a better performance in fire mechanical properties by introducing these novel fillers.

4. Conclusions

To tackle the challenge of the flammability of biobased epoxy resin systems, a novel cobalt-based nano-micro hybrid filler was proposed, designed, and prepared in this work. When the ratio of CNH to APP was 7:3 when added to epoxy, it demonstrated the best flame-retardant performance, as indicated by LOI, UL 94 and CCT results. It is worth noting that when the GFRCs, fabricated using the flame-retarded resin, were observed with suppressed intumescent effects compared to that of resin, which was proposed to be derived from the interference of glass fibers. With no fire damage, the 14APP-6CNH/APP showed a better axial tensile strength due to the global failure redistribution mechanism opposing the local one observed in the 20APP/GFRP laminate. Under simultaneous axial static force loading and fire damage, the composite with optimized matrix material also protects itself from mechanical failure by delaying failure time by more than 15 %.

CRediT authorship contribution statement

Deyi Wang: Writing – review & editing, Supervision, Methodology, Conceptualization. **Carlos González:** Writing – original draft, Supervision, Methodology. **Robert Crouse:** Writing – review & editing, Methodology. **Xiang Ao:** Writing – original draft, Methodology, Formal analysis, Data curation, Conceptualization.

Declaration of Competing Interest

The authors declare that they have no known competing financial interests or personal relationships that could have appeared to influence the work reported in this paper.

Data availability

Data will be made available on request.

Acknowledgements

This research is partly funded by China Scholarship Council under Grant CSC No. 202006630011.

Appendix A. Supporting information

Supplementary data associated with this article can be found in the online version at doi:10.1016/j.conbuildmat.2024.136922.

References

[1] K. Daehn, R. Basuhi, J. Gregory, M. Berlinger, V. Somjit, E.A. Olivetti, Innovations to decarbonize materials industries, Nat. Rev. Mater. 7 (4) (2021) 275–294.
[2] V.G. Zuin, K. Kummerer, Chemistry and materials science for a sustainable circular polymeric economy, Nat. Rev. Mater. 7 (2) (2022) 76–78.
[3] G. Hayes, M. Laurel, D. MacKinnon, T. Zhao, H.A. Houck, C.R. Becer, Polymers without petrochemicals: sustainable routes to conventional monomers, Chem. Rev. 123 (5) (2023) 2609–2734.
[4] R.M. Cywar, N.A. Rorrer, C.B. Hoyt, G.T. Beckham, E.Y.X. Chen, Bio-based polymers with performance-advantaged properties, Nat. Rev. Mater. 7 (2) (2021) 83–103.
[5] J. Liu, S. Wang, Y. Peng, J. Zhu, W. Zhao, X. Liu, Advances in sustainable thermosetting resins: from renewable feedstock to high performance and recyclability, Prog. Polym. Sci. 113 (2021) 101353.
[6] X.-L. Zhao, Y.-D. Li, J.-B. Zeng, Progress in the design and synthesis of biobased epoxy covalent adaptable networks, Polym. Chem. 13 (48) (2022) 6573–6588.
[7] H.-X. Niu, X. Wang, L. Song, Y. Hu, Progress on intrinsically flame-retardant bio-based epoxy thermosets, Acta Polym. Sin. 53 (8) (2022) 894–905.
[8] J. Wan, J. Zhao, X. Zhang, H. Fan, J. Zhang, D. Hu, P. Jin, D.-Y. Wang, Epoxy thermosets and materials derived from bio-based monomeric phenols: Transformations and performances, Prog. Polym. Sci. 108 (2020) 101287.
[9] X. Wang, W. Guo, L. Song, Y. Hu, Intrinsically flame retardant bio-based epoxy thermosets: a review, Compos. Part B 179 (2019) 107487.
[10] R. Auvergne, S. Caillol, G. David, B. Boutevin, J.P. Pascault, Biobased thermosetting epoxy: present and future, Chem. Rev. 114 (2) (2014) 1082–1115.
[11] E.A. Baroncini, S. Kumar Yadav, G.R. Palmese, J.F. Stanzione, Recent advances in bio-based epoxy resins and bio-based epoxy curing agents, J. Appl. Polym. Sci. 133 (45) (2016).
[12] X.-H. Shi, X.-L. Li, Y.-M. Li, Z. Li, D.-Y. Wang, Flame-retardant strategy and mechanism of fiber reinforced polymeric composite: a review, Compos. Part B 233 (2022) 109663.
[13] X. Ao, A. Vázquez-López, D. Mocerino, C. González, D.-Y. Wang, Flame retardancy and fire mechanical properties for natural fiber/polymer composite: a review, Compos. Part B 268 (2024) 111069.
[14] X.-F. Liu, Y.-F. Xiao, X. Luo, B.-W. Liu, D.-M. Guo, L. Chen, Y.-Z. Wang, Flame-retardant multifunctional epoxy resin with high performances, Chem. Eng. J. 427 (2022) 132031.
[15] B.K. Kandola, F. Magnoni, J.R. Ebdon, Flame retardants for epoxy resins: application-related challenges and solutions, J. Vinyl Addit. Technol. 28 (1) (2022) 17–49.
[16] Y. Yang, D.-Y. Wang, R.-K. Jian, Z. Liu, G. Huang, Chemical structure construction of DOPO-containing compounds for flame retardancy of epoxy resin: a review, Prog. Org. Coat. 175 (2023) 107316.
[17] A. Bifulco, C.D. Varganici, L. Rosu, F. Mustata, D. Rosu, S. Gaan, Recent advances in flame retardant epoxy systems containing non-reactive DOPO based phosphorus additives, Polym. Degrad. Stab. 200 (2022) 109962.
[18] T. Chu, Y. Lu, B. Hou, P. Jafari, Z. Zhou, H. Peng, S. Huo, P. Song, The application of ammonium polyphosphate in unsaturated polyester resins: a mini review, Polym. Degrad. Stab. 225 (2024) 110796.
[19] Morgan A.B. Non-halogenated flame retardant handbook: John Wiley & Sons; 2021.
[20] Z.-B. Shao, X. Song, T.-C. Wang, J. Cui, W. Ye, B. Xu, D.-Y. Wang, Facile Fabrication of organic zirconium/inorganic phosphorus complex for super-efficiently flame-retardant epoxy resin, Compos. Commun. 36 (2022) 101360.
[21] K. Song, Y.-T. Pan, J. Zhang, P. Song, J. He, D.-Y. Wang, R. Yang, Metal–Organic Frameworks–based flame-retardant system for epoxy resin: a review and prospect. Chem. Eng. J. 468 (2023) 143653.
[22] J. Zhang, Z. Li, X.L. Qi, D.Y. Wang, Recent progress on metal-organic framework and its derivatives as novel fire retardants to polymeric materials, Nano Micro Lett. 12 (1) (2020) 173.
[23] J. Zhang, X. Ao, X. Zhang, R. Wang, X. Jin, W. Ye, B. Xu, D.-Y. Wang, Construction of nanomaterials based on molybdenum disulfide decorated onto a metal–organic framework (UiO-66) to improve the fire retardancy of epoxy, ACS Appl. Nano Mater. 5 (12) (2022) 17731–17740.
[24] B. Hou, W. Zhang, H. Lu, K. Song, Z. Geng, X. Ye, Y.T. Pan, W. Zhang, R. Yang, Multielement flame-retardant system constructed with metal poss-organic frameworks for epoxy resin, ACS Appl. Mater. Interfaces 14 (43) (2022) 49326–49337.
[25] X. Song, B. Hou, Z. Han, Y.-T. Pan, Z. Geng, L. Haurie Ibarra, R. Yang, Dual nucleation sites induced by ZIF-67 towards mismatch of polyphosphazene hollow sub-micron polyhedrons and nanospheres in flame retardant epoxy matrix, Chem. Eng. J. 470 (2023) 144278.
[26] K. Song, B. Hou, Z. Ur Rehman, Y.-T. Pan, J. He, D.-Y. Wang, R. Yang, Sloughing" of metal-organic framework retaining nanodots via step-by-step carving and its flame-retardant effect in epoxy resin, Chem. Eng. J. 448 (2022).
[27] X. Ao, J. Xiao, J. Hobson, J. de la Vega, G. Yin, M.L. Puertas Cuadron, A. Esteban Cubillo, C. González, D.-Y. Wang, Bilayer coating strategy for glass fiber reinforced polymer composites toward superior fire safety and post-fire mechanical properties, Compos. Commun. 44 (2023) 101763.
[28] R. Samiee, S. Montazeri, B. Ramezanzadeh, M. Mahdavian, Ce-MOF nanorods/aluminum hydroxide (AlTH) synergism effect on the fire-retardancy/smoke-release and thermo-mechanical properties of a novel thermoplastic acrylic intumescent composite coating, Chem. Eng. J. 428 (2022) 132533.
[29] Y.T. Pan, L. Zhang, X. Zhao, D.Y. Wang, Interfacial engineering of renewable metal organic framework derived honeycomb-like nanoporous aluminum hydroxide with tunable porosity, Chem. Sci. 8 (5) (2017) 3399–3409.
[30] B. Schartel, T.R. Hull, Development of fire-retarded materials—interpretation of cone calorimeter data, Fire Mater. 31 (5) (2007) 327–354.
[31] Hu Y., Wang X. Flame Retardant Polymeric Materials: A Handbook: CRC Press; 2019.
[32] J. Alongi, Z. Han, S. Bourbigot, Intumescence: tradition versus novelty. A comprehensive review, Prog. Polym. Sci. 51 (2015) 28–73.

[33] A. Sandinge, P. Blomqvist, M. Rahm, A modified specimen holder for cone calorimeter testing of composite materials to reduce influence from specimen edges, Fire Mater. 46 (1) (2021) 80–94.
[34] A.P. Mouritz, S. Feih, E. Kandare, Z. Mathys, A.G. Gibson, P.E. Des Jardin, S. W. Case, B.Y. Lattimer, Review of fire structural modelling of polymer composites, Compos. Part A 40 (12) (2009) 1800–1814.
[35] Babrauskas V. Ignition handbook: principles and applications to fire safety engineering, fire investigation, risk management and forensic science: Fire Science Publishers; 2003.
[36] B. Perret, B. Schartel, K. Stöß, M. Ciesielski, J. Diederichs, M. Döring, J. Krämer, V. Altstädt, A new halogen-free flame retardant based on 9,10-Dihydro-9-oxa-10-phosphaphenanthrene-10-oxide for epoxy resins and their carbon fiber composites for the automotive and aviation industries, Macromol. Mater. Eng. 296 (1) (2010) 14–30.
[37] B. Perret, B. Schartel, K. Stöß, M. Ciesielski, J. Diederichs, M. Döring, J. Krämer, V. Altstädt, Novel DOPO-based flame retardants in high-performance carbon fibre epoxy composites for aviation, Eur. Polym. J. 47 (5) (2011) 1081–1089.
[38] L. Zhang, Y. Ou, D.Y. Wang, Surface functionalization of carbon fabric towards high-performance epoxy composites via enhanced fiber–matrix interfacial strength and intergrowth charring behavior, Express Polym. Lett. 15 (6) (2021) 503–514.